COMPARISON OF PHOTOPHYSICAL AND PHOTOCHEMICAL BEHAVIOR OF FULLERENE DERIVATIVES WITH UNFUNCTIONALIZED FULLERENES

L. Juha[1,4], V. Hamplová[1], Z. Pokorná[1], J. Kodymová[1], O. Špalek[1], J. Krása[1], K. Lang[2], P. Kubát[3], F. P. Boody[4], E. Koudoumas[5], S. Couris[5], I. Stibor[6], T. Gareis[7], O. Köthe[7], J. Daub[7]

1. Institute of Physics, Academy of Sciences of the Czech Republic, Na Slovance 2, 180 40 Prague 8, Czech Republic (e-mail: juha@fzu.cz)
2. Institute of Inorganic Chemistry, Academy of Sciences of the Czech Republic, Pelléova 24, 160 00 Prague 6, Czech Republic
3. J. Heyrovský Institute of Physical Chemistry, Academy of Sciences of the Czech Republic, Dolejškova 3, 182 23 Prague 8, Czech Republic
4. Regensburg Institute of Technology, P. O. Box 120327, D-93025 Regensburg, Germany
5. Institute of Electronic Structure and Laser, Foundation for Research and Technology - Hellas, P. O. Box 1527, Heraklion 71110, Crete, Greece
6. Prague Institute of Chemical Technology, Technická 5, 166 28 Prague 6, Czech Republic
7. Institute of Organic Chemistry, University of Regensburg, D-93040 Regensburg, Germany

The photophysical properties of several dihydrofullerenes were measured in toluene solutions. A reduction of the singlet oxygen quantum yields Φ_Δ (less than 15 %) due to functionalization was found only for the pyrene and chlorine containing derivatives. Φ_Δ is not affected by attached cyclohexanol to C_{70} or C_{60} within experimental error. C_{60} derivatives exhibit larger optical nonlinearities than unfunctionalized C_{60}, whereas the corresponding C_{70} derivatives have slightly smaller nonlinearities than C_{70}. The photochemical stability was determined for pulsed laser (308 nm) and daylight irradiation in toluene solution. It was found that the photostability when irradiated by 308 nm radiation decreases with functionalization; the decrease being more profound for C_{60} than for C_{70}. Under daylight irradiation the derivatives exhibit high stability with the exception of the chlorine containing derivative.

INTRODUCTION

Discovery of an efficient method for preparation of macroscopic amounts of C_{60} and C_{70} fullerenes in 1990 (1) has allowed not only the study of fullerenes themselves but has also been followed by the successful syntheses of various fullerene derivatives, e.g. (2), as well as extensive research on the properties of these, rapidly growing in number,

compounds. Scientific activity devoted to the study of the photophysical and photochemical properties of fullerene derivatives now appears (3) to exceed that devoted to the study of unfunctionalized C_{60} and C_{70}, e.g. (4). Early on it was found that, by functionalization of the fullerene cage, its chemical and physical properties could be dramatically changed. A promising opportunity exists for the utilization of fullerene-based materials for many applications because it is possible, due to functionalization, to improve on some of the undesirable properties of fullerenes (e.g. weak absorption in visible region, poor solubility in polar solvents, etc.) while maintaining their desirable properties (e.g. high quantum yields of triplet states, singlet oxygen, relatively good photochemical stability, etc.). The main task is to design suitable functionalizations which will not cause the desirable properties of the cage to disappear.

At the fundamental level, the main goal of the study of fullerene derivatives is understanding how functionalization affects the electronic structure of fullerene and thus influences its photophysical and photochemical properties. Knowledge obtained in the framework of such study should be useful for the molecular design of fullerene-based compounds which exhibit properties tailored for the following applications:

Construction of a **dry solid-gas singlet oxygen generator** (5), for which fullerene derivatives are required with strong absorption in the visible, high singlet oxygen quantum yields, good photochemical stability, and which allow efficient molecular oxygen transport through their solid layers. Although this generator is first destined to be a part of an oxygen-iodine laser (4f, 6), it might also be used in biomedical and chemical laboratories.

Successful use of fullerene derivatives as **sensitizers in photodynamic therapy of cancer** and as **molecular tools for photo-induced sequence-specific DNA cleavage** (7) require their water solubility, strong absorption in the Vis/NIR region, high quantum yield of singlet oxygen, good photochemical stability, and nontoxicity in the ground state.

Fullerene derivatives will be used as **sensitizers of photooxygenation reactions in laboratories** (8) **and photochemical facilities utilizing solar energy** (9), if they can be made to strongly absorb visible radiation, produce singlet oxygen with high quantum yields, are stable under long-term irradiation, and have good solubility in common solvents.

If the triplet-triplet absorption spectra of some derivatives should show higher absorption coefficients in the visible than unfunctionalized fullerenes, they might be used as **optical limiters**.

For our experiments devoted to the study of the photophysical and photochemical properties of fullerene derivatives and to their comparison with unfunctionalized fullerenes, we have chosen compounds (Fig. 1) synthesized at the Institute of Organic Chemistry of the University of Regensburg (10). Among the large numbers of functionalization methods for fullerenes, cycloaddition reactions seem to be the most powerful tools (11). Special attention must be drawn to the method of Rubin et al. (12), which includes the Diels-Alder addition of an electron rich silyle enole ether to the

acceptor moiety of fullerene. In an expansion of this original concept, we have studied the use of modified enole ethers to introduce various groups to fullerene (10). The synthesis implies the aldole condensation of an aldehyde to the corresponding enone and modification to a silyl enole ether by use of Danishefski's method (13).

SINGLET OXYGEN PRODUCTION

Fullerenes produce singlet oxygen in large quantities with quantum yields close to unity (4a-d) and exhibit good photochemical stability (4a, b, f, n). The presence of a tailored side chain can significantly affect the production of singlet oxygen. It has been found, for multiply-functionalized derivatives, that increasing perturbation of fullerene's π-system reduces $^1O_2$ quantum yields (3a, b, g, h). Monofunctionalization has less apparent effect, since the photochemical properties of fullerene moiety remain intact while the optical, photochemical and electrochemical properties of a side chain become more dominant.

We have determined the relative singlet oxygen quantum yields Φ_Δ for a set of fullerene derivatives **1 - 6** in aerated toluene at excitation wavelengths of 308 nm and 410 nm using time-resolved near-IR luminescence measurement (Table I). The decay of 1270-nm $^1O_2$ luminescence (14) was monoexponential throughout. Details of the apparatus and data handling procedures have been given elsewhere (15). The Φ_Δ were estimated from the energy dependence of the zero-time amplitude of the signal intensity (Fig. 2). They are expressed relative to C_{60}, whose Φ_Δ is arbitrarily taken to be 1.00. All of the air-saturated toluene solutions were optically matched to give absorbances of 0.241 $\pm$ 0.003 and 0.289 $\pm$ 0.003 in a 1-cm cell at 308 and 410 nm, respectively. Multiphotonic processes are the cause of the negative deviations from linearity in the zero-intensity amplitude vs. laser energy plots. For this reason, only the linear region (usually energies from 30 up to 120 μJ) was considered for the evaluation of Φ_Δ (Table I). All compounds were stable under the conditions used for these measurements.

Comparing the Φ_Δ of C_{60} and **6** it appears that the cyclohexanol side chain does not affect the production of $^1O_2$. This is in a good agreement with Anderson *et al.* (3a), although we have used different excitation wavelengths and solvents. Compound **5** is the worst singlet oxygen producer of **4 - 6**. The presence of a chlorine atom within the cyclohexane side chain probably influences spin-orbit coupling and consequently limits the production of $^1O_2$. We have also synthesized compound **4** , an analog of **6**, with C_{70}. Comparing **4** and C_{70}, no effect of the cyclohexanol side chain on Φ_Δ has been observed. This behavior, similar to the results for C_{60} and **6**, has not yet been reported. Comparison of the Φ_Δ for **2** and **3** reflect the effect of the moieties phenylanthracene (**2**) and pyrene (**3**) on $^1O_2$ production, since the moieties cyclohexanon (**2**) and esterificated cyclohexanol (**3**) are closely bound to C_{60} and thus do not affect Φ_Δ. Phenylanthracene moiety can behave independently as a $^1O_2$ producer, considering the fact that part of the incident radiation is directly absorbed by this polycyclic aromatic hydrocarbon (PAH) moiety. We cannot, however, confirm this independent behavior within **2** since the combination of the minor

absorption of the incident radiation by phenylanthracene moiety (up to 12 %) and its high $^1O_2$ quantum yield of about 0.9 would not change Φ_Δ more than the experimental error. Thus, within the experimental error, compound **2** exhibits equal Φ_Δ to C_{60} (the same holds for **1** with pyrene moiety and C_{70}). On the other hand, compound **3** exhibits reduced Φ_Δ when compared with C_{60}. This can be interpreted as a result of the C_{60}-pyrene electronic interaction. It is interesting to point out that for compound **1** - the C_{70} analog - no effect of pyrene on Φ_Δ has been observed (Table I). Work on energy transfer from PAH to fullerene moiety and the validity of Kasha's rule is in progress.

Table I. Singlet oxygen quantum yields Φ_Δ in aerated toluene, normalized to C_{60}, at two excitation wavelengths λ_{exc}

Compound	Φ_Δ (λ_{exc} = 308 nm)	Φ_Δ (λ_{exc} = 410 nm)
C_{60}	1.00±0.06	1.00±0.05
C_{70}	0.96±0.08	1.01±0.05
1	0.93±0.08	0.92±0.05
2	0.88±0.06	1.00±0.05
3	0.74±0.06	0.86±0.04
4	-	0.95±0.06
5	-	0.89±0.04
6	-	0.95±0.05

NONLINEAR OPTICAL RESPONSE

For the measurement of the optical nonlinearities, a degenerate four wave mixing (DFWM) based self-diffraction configuration was used (16). In this configuration, two input beams with wavevectors $\mathbf{k}_1$ and $\mathbf{k}_2$, respectively, interact through nonlinear polarization in the sample to produce two parametric signals in the directions $\mathbf{k}_3=2\mathbf{k}_1-\mathbf{k}_2$ and $\mathbf{k}_4=2\mathbf{k}_2-\mathbf{k}_1$. These signals correspond to a four wave mixing process related to an effective third-order nonlinear susceptibility $\chi_{eff}^{(3)}$, and are given by an equation of the form:

$$I_s \propto |\chi_{eff}^{(3)}|^2 \times (I_1^2 \times I_2) \times \{[\alpha L \times \exp(\alpha L/2)] / [1 - \exp(-\alpha L)]\}^{-2} \qquad [1]$$

where I_s is the intensity of generated signal, I_1 and I_2 are the incident radiation intensities, L is the sample thickness and α is the absorption coefficient, the last term being a correction related to the linear absorption of the samples.

The second harmonic of a Nd: YAG laser delivering 10-ns pulses at 532 nm was used as the pump source. The output was divided into two beams, which were focused on the sample cell with a 15 cm focal length lens. The angle between the two beams was approximately 1°, and the beam diameter at the focal plane was measured to be around

120 μm. A photomultiplier was used to detect the signal, which was averaged over 500 laser shots with a fast digital storage oscilloscope (LECROY 9450, 350 MHz). Six samples (C_{60}, C_{70}, **1**, **3**, **4** and **6** in toluene) were prepared with a concentration of about 1 mM. Their absorption spectra were measured with a Perkin-Elmer spectrophotometer and checked before and after irradiation, in order to verify that no photodegradation of the samples had occurred.

For input intensities of about a few hundred kW-cm^{-2}, parametric signals in the directions $\mathbf{k_3=2k_1-k_2}$ and $\mathbf{k_4=2k_2-k_1}$ appeared for all samples. The intensity dependence of the signal $\mathbf{k_3}$ is shown in Fig. 3a for C_{60}, **3**, and **6** and Fig. 3b for C_{70}, **1**, and **4**. In all cases, the signal $\mathbf{k_3}$ increases following a third-order power law, proving that this is related to a four wave mixing process. As can be seen, C_{60} derivatives are characterized by higher optical nonlinearities when compared with unfunctionalized C_{60}, whereas the corresponding C_{70} derivatives have slightly smaller optical nonlinearities than C_{70}. The optical nonlinearities of C_{70}, **1** and **4** are much greater than those of the corresponding C_{60} derivatives (see Fig.3).

PHOTOCHEMICAL STABILITY

The fullerene derivatives **1** - **6** and the unfunctionalized fullerenes C_{60} and C_{70} were irradiated in aerated toluene with XeCl laser light (308 nm) in quartz cells and with daylight in glass vials. The chemical changes were observed by means of UV/Vis spectrophotometry and high performance liquid chromatography (HPLC).

A comparison of the UV/Vis spectra of the irradiated solutions (the selected spectra can be seen in Figs 4 - 6) indicates that all of the derivatives **1** - **6** seem to be less stable than the corresponding unfunctionalized fullerenes, under the given irradiation conditions. The chromatograms allow estimation of the decomposition yields (Fig. 7). The decomposition yields of fullerene derivatives **1** - **6** are higher for each derivative than for the corresponding unfunctionalized fullerene and the difference between the functionalized and unfunctionalized fullerene is significantly higher for C_{60} than for C_{70}. The first finding had been expected, based on the results obtained for the epoxide $C_{60}O$ by other groups (3 l, m) But, the second finding is surprising and, together with the high Φ_Δ (Table I), looks to be very promising for the prospective applications of C_{70} derivatives.

Although the derivative peaks in the chromatograms of irradiated solutions of derivatives containing PAH moiety (**1-3**) completely disappeared above a given number of XeCl laser shots (6000, 5000, and 2000 for **1**, **2** and **3**, respectively), in the corresponding absorption spectra (see for example Figs. 4 and 6) bands assigned to pyrene (316 nm, 330 nm , and 345 nm) and phenylanthracene (366 nm and 387 nm) can still be seen. This indicates that the PAH part of dyads **1-3** survived substantial decomposition of the fullerene cage. Since the photodecomposition efficiencies are quite similar for the derivatives containing PAH moiety (**1-3**), as well as for the simple dihydrofullerenes (**4-6**), it seems more likely that the PAH molecules observed in the deeply irradiated solutions

are residua from photoinduced breakdown of the fullerene part of the dyad rather than species split off from the dyad by spacer photodissociation. In this respect further progress is not possible without identification of decomposition products by means of advanced separation and analytical techniques.

A lift of the whole spectrum during irradiation (Figs 4 - 6), caused by the formation of a dark-brown precipitate in the irradiated solution, has been observed not only in solutions of an unfunctionalized fullerenes (for which this phenomenon already has been described, for lamp (4i) and laser (17) induced photolysis) but also for **1** - **6**. C_{70} and its derivatives produce this solid phase with higher yields than C_{60} and its derivatives. Characterization of the fine solid particles formed during irradiation is in progress using appropriate methods (dynamic light scattering, esr, photoacoustic and Raman spectroscopy). The findings presented here and further investigation of the observed phenomenon are topical because of the proposed mechanisms of precipitate formation recently published by Yang and Hwang (18).

As can be seen in Fig. 5, during the irradiation of **5** a broad band with a maximum at 490 nm appeared which has not been observed in the spectra of other compounds. It could indicate the presence of unknown photolysis product, which we are now trying to identify (by means of gel permeation chromatography and then by FAB-mass and IR spectroscopy of isolated products). This finding also reiterates the difference of this chlorine containing derivative from the others studied (compare its Φ_Δ in Table I and note its unusual behavior under daylight irradiation, see below).

A three-week irradiation of the toluene solutions of **1** - **4** and **6** by daylight did not lead to any observable chemical changes, in comparison with the control solutions kept in the dark. These results agree with the conclusion reached for laser-induced photolysis, that the derivatives are less, but not dramatically less, photochemically stable than unfunctionalized C_{60} and C_{70}. However, **5** irradiated under the same conditions, showed completely different photochemical behavior. The chromatograms shown in Fig. 8 (two peaks with retention times 410 and 435 s are assigned to the isomers of **5** depicted in Fig. 1 as **7a** and **7b**) testify that, after the given irradiation time, this compound was fully decomposed. Neither the yield of the XeCl laser-induced photolysis of this compound (see Fig. 7) nor the chromatograms of the irradiated solutions (Fig. 9) indicate any exceptional photochemical reactivity of **5**. Only in the UV/Vis spectra can something different from the other derivatives be seen, as mentioned above. The presence of chlorine in the molecule **5** likely causes the observed reactivity during long-term low-intensity irradiation. In order to better understand the processes we are conducting experiments with different irradiation wavelengthes and intensities and using other techniques for product identification.

CONCLUSIONS

Functionalization of C_{60} by cyclohexanol (**6**) and phenyl anthracene (**2**) has no effect on Φ_Δ. On the other hand, the pyrene derivative **3** has reduced singlet oxygen quantum yield in contrast to the corresponding C_{70} analog **1**. The chlorine containing derivative **5** exhibits lower production of $^1O_2$ than unfunctionalized C_{60}.

Φ_Δ of **1** and **4** are not affected by attached cyclohexanol (**4**) and pyrene esterificated cyclohexanole (**1**) within experimental error when compared to unfunctionalized C_{70}.

C_{60} derivatives **3** and **6** exhibit larger optical nonlinearities than unfunctionalized C_{60}, whereas the corresponding C_{70} derivatives have slightly smaller optical nonlinearities than the C_{70} derivatives **1** and **4**. The optical nonlinearities of C_{70}, **1** and **4** are much greater than these of C_{60} derivatives.

The derivatives **1** - **6** are less stable under irradiation by XeCl laser radiation ($\lambda = 308$ nm; $I = 3$ MW cm^{-2}) in aerated toluene than the corresponding unfunctionalized fullerene. Derivatives of C_{70} are more stable than derivatives of C_{60}.

Derivatives **1** - **4** and **6** show very good stability when exposed to daylight in aerated toluene for three weeks. On the other hand **5** completely decomposed while the same solution, kept in the dark for the same period, stays unchanged.

ACKNOWLEDGEMENT

Samples of C_{60} and C_{70} were generously provided by Dr. ter Meer, Hoechst AG, Frankfurt am Main (Germany).

REFERENCES

1. W. Krätschmer, L. D. Lamb, K. Fostiropoulos, D. R. Huffman, Nature, **318**, 354 (1990).
2. a) R. Taylor and D. R. M. Walton, Nature, **363**, 685 (1993).
   b) A. Hirsch, The Chemistry of the Fullerenes, Georg Thieme Verlag, Stuttgart-New York (1994).
   c) The Chemistry of Fullerenes, R. Taylor, Editor, World Scientific, Singapore-New Jersey-London-Hong Kong (1995).
   d) F. Diederich and C. Thilgen, Science, **271**, 317 (1996).
3. a) J. L. Anderson, Y.-Z. An, Y. Rubin, C. S. Foote, J. Am. Chem. Soc., **116**, 9763 (1994).
   b) C. S. Foote, in Physics and Chemistry of the Fullerenes, K. Prassides, Editor, p. 79, Kluwer Academic Publishers, Dordrecht-Boston-London (1994).
   c) Y. Nakamura, T. Minowa, S. Tobita, H. Shizuka, J. Nishimura, J. Chem. Soc., Perkin Trans. 2, 2351 (1995).
   d) R. M. Williams, J. M. Zwier, J. W. Verhoeven, J. Am. Chem. Soc., **117**, 4093

(1995).
e) R. V. Bensasson, E. Bienvenue, J.-M. Janot, S. Leach, P. Seta, D. I. Schuster, S. R. Wilson, H. Zhao, Chem. Phys. Lett., **245**, 556(1995).
f) R. V. Bensasson, T. J. Hill, E. J. Land, S. Leach, D. J. McGarvey, T. G. Truscott, J. Ebenhoch, M. Gerst, C. Rüchardt, Chem.Phys., **215**,111(1997).
g) F. Cardullo, L. Isaacs, F. Diederich, J.-P. Gisselbrecht, C. Boudon, M. Cross, Chem.Commun., 797(1996).
h) T. Hamano, K. Okuda, T. Mashino, M. Hirobe, K. Arakane, A. Ryu, S. Mashiko, T. Nagano, Chem. Commun., 21 (1997).
i) D. Kaciuskas, S. Lin, G. R. Seely, A. L. Moore, T. A. Moore, D. Gust, T. Drovetskaya, C. A. Reed, P. D. W. Boyd, J.Phys.Chem., **100**, 15926 (1996).
j) H. Imahori, K. Hagiwara, M. Aoki, T. Akiyama, S. Tanigushi, T. Okada, M. Shirakawa, Y. Sakata, J. Am.Chem. Soc., **118**, 11771 (1996).
k) D. M. Guldi and K.-D. Asmus, J. Phys. Chem., **A101**, 1472 (1997).
l) D. Heymann and L. P. F. Chibante, Chem. Phys. Lett., **207**, 339 (1993).
m) J.-P. Deng, D.-D. Ju, G.-R. Her, C.-Y. Mou, C.-J. Chem, Y.-Y. Lin, C.-C. Han, J. Phys. Chem., **97**, 11575 (1993).
n) R. D. Beck, P. Weis, A. Hirsch, I. Lamparth, J. Phys. Chem., **98**, 9683 (1994).
o) Y.-Z. An, A. L. Viado, M.-J. Arce, Y. Rubin, J. Org. Chem., **60**, 8330 (1995).
p) Z. Li and P. B. Shevlin, J. Am. Chem. Soc., **119**, 1149 (1997).
4. a) J. W. Arbogast, A. P. Darmayan, C. S. Foote, Y. Rubin, F. N. Diederich, M. A. Alvarez, S. J. Anz, R. L. Whetten, J.Phys.Chem., **95**,11(1991).
b) J. W. Arbogast, C. S. Foote, J. Am. Chem. Soc., **113**, 8886 (1991).
c) R. R. Hung, J. J. Grabowski, J. Phys. Chem., **95**, 6073 (1991).
d) R. R. Hung, J. J. Grabowski, Chem. Phys. Lett., **192**, 249 (1992).
e) N. M. Dimitrijevic, P. V. Kamat, J. Phys. Chem., **96**, 4811(1992).
f) G. Black, E. Dunkle, E. A. Dorko, L. A. Schlie, J. Photochem. Photobiol., **A70**, 147 (1993).
g) R. M. Williams, J. W. Verhoeven, Spectrochim.Acta, **50A**, 251 (1994).
h) C. S. Foote, Top. Curr. Chem., **169**,347(1994).
i) R. Taylor, J. P. Parsons, A. G. Avent, S. P. Rannard, T. J. Dennis, J. P. Hare, H. W. Kroto, D. R. M. Walton, Nature, **351**, 277 (1991).
j) M. Gevaert, P. V. Kamat, J. Chem. Soc., Chem.Commun., 1470 (1992).
k) S. C. O'Brien, J. R. Heath, R. F. Curl, R. E. Smalley, J. Chem. Phys., **88**, 220 (1988).
l) R. Taylor, Phil.Trans. R. Soc. Lond., **A343**, 101 (1993).
m) L. Juha, V. Hamplová, P. Engst, P. Kubát, E. Koudoumas, S. Couris, J. Phys. Chem., **99**, 8200 (1995).
n) L. Juha, V. Hamplová, P. Kubát, E. Koudoumas, S. Couris, Chem. Phys. Lett., **231**,314 (1994).
5. W. C. Eisenberg, Adv. Oxygen. Proc., **3**, 71 (1991).
6. J. Kodymová, O. Špalek, S. Lunák, L. Juha, V. Hamplová, Proc. SPIE, **2767**, 245 (1996).
7. a) H. Tokuyama, S. Yamago, E. Nakamura, T. Shiraki, Y. Sugiura, J. Am. Chem. Soc.

115, 7918 (1993).
b) A. S. Boutorine, H. Tokuyama, M. Takasugi, H. Isobe, E. Nakamura, C. Helene Angew. Chem. Int. Ed. Engl., **33**, 2462 (1993)
c) E. Nakamura, H. Tokuyama, S. Yamago, T. Shiraki, Y. Sugiura, Bull. Chem. Soc. Jpn., **69**, 2143 (1996).
d) A. J. Jensen, S. R. Wilson, D. I. Schuster, Bioorg. Med. Chem., **4**, 767 (1996).
8. H. Tokuyama, E. Nakamura, J.Org.Chem., **59**, 1135 (1994).
9. P. Esser, B. Pohlmann, H.-D. Scharf, Angew. Chem. Int. Ed. Engl., **33**, 2009 (1994).
10. a) T. Gareis, Diploma thesis, University of Regensburg, Regensburg (1994).
b) T. Gareis, PhD thesis, University of Regensburg, Regensburg (1997).
c) T. Gareis, O. Köthe, E. Beer, J. Daub, Proc. Electrochem. Soc., **96-10,** 1244 (1996)
d) O. Köthe, Diploma thesis, University of Regensburg, Regensburg (1996).
11. a) X. Zang, C. S. Foote, J. Am. Chem. Soc., **117**, 4271 (1995).
b) M. Prato, M. Maggini, G. Scorrano, V. Lucchini, J. Org. Chem., **58**, 3613 (1993).
c) F. Wudl, Acc. Chem. Res., **25**, 157 (1993).
d) M. Prato, T. Suzuki, H. Foroudioan, Q. Li, K. Khemani, F.Wudl, J. Am. Chem. Soc., **115,** 1594 (1993).
e) S. I. Khan, A. M. Oliver, M. N. Paddon-Row, Y. Rubin, J. Am. Chem. Soc., **115,** 4919 (1993).
f) E. Beer, M. Feuerer, A. Knorr, A. Mirlach, J. Daub, Angew. Chem. Int. Ed. Engl. **33**, 1087 (1994).
12. Y.-Z. An, J. L. Anderson, Y. Rubin, J. Org. Chem., **58**, 4799 (1993).
13. see literature cited in M. E. Jung, A. McCombs, Y. Takeda, Y.-G. Pan, J. Am. Chem Soc., **103**, 6677 (1981).
14. a) A. A. Krasnovski, Biofizika, **21**, 748 (1975).
b) M. Kasha, A. U. Khan, Proc. Natl. Acad. Sci. USA, **76**, 6047 (1979).
c) P. R. Ogilby, C. S. Foote, J. Am. Chem. Soc., **104**, 2070 (1982).
15. P. Kubát, Z. Zelinger, M. Jirsa, Radiat. Res., in press.
16. a) A Maruani, J. L. Oudar, E. Batifol, D.S. Chemla, Phys. Rev. Lett., **41,** 1372 (1978).
b) L.H. Acioli, A.S.L. Gomes, J.R. Rios Leite, C. B. De Araujo, IEEE J. Quant. Electr., **26**, 1277 (1990).
c) S. Couris, E. Koudoumas, F. Dong, S. Leach, J. Phys. **B29**, 5033 (1996).
17. L. Juha, J. Krása, L. Láska, V. Hamplová, L. Soukup, P. Engst, P. Kubát, Appl. Phys., **B57**, 83 (1993).
18. C. C. Yang, K. Ch. Hwang, J. Am. Chem. Soc., **118**, 4693 (1996).

Fig. 1. Formulae of the fullerene derivatives studied.

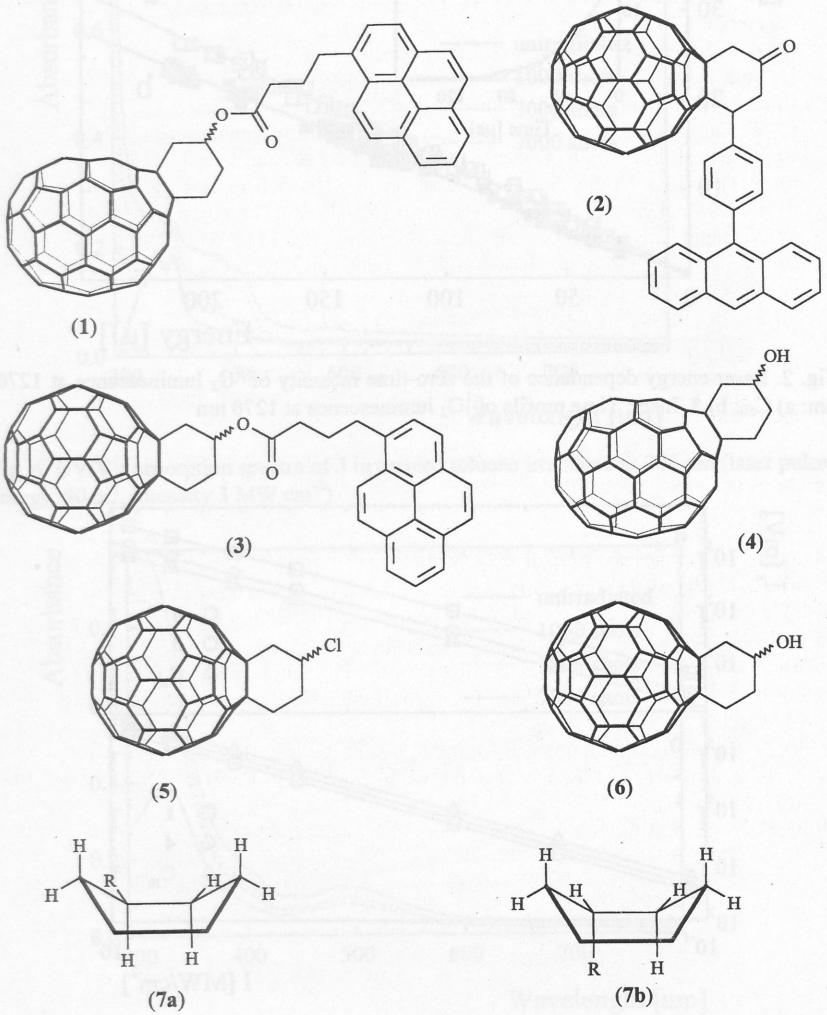

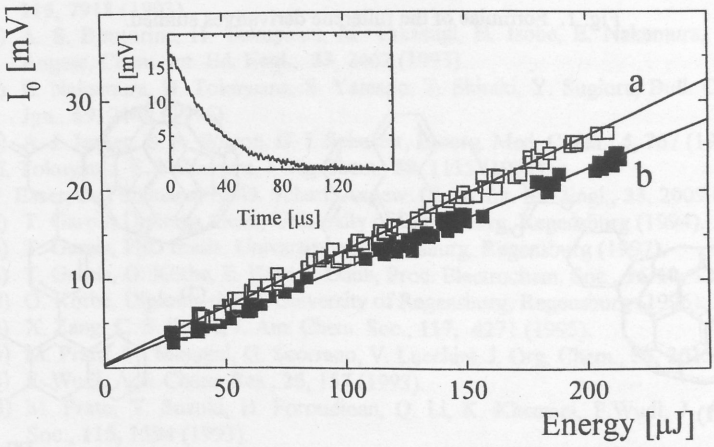

Fig. 2. Laser-energy dependence of the zero-time intensity of $^1O_2$ luminescence at 1270 nm: a) C_{60}; b) **3**. Inset: Time profile of $^1O_2$ luminescence at 1270 nm

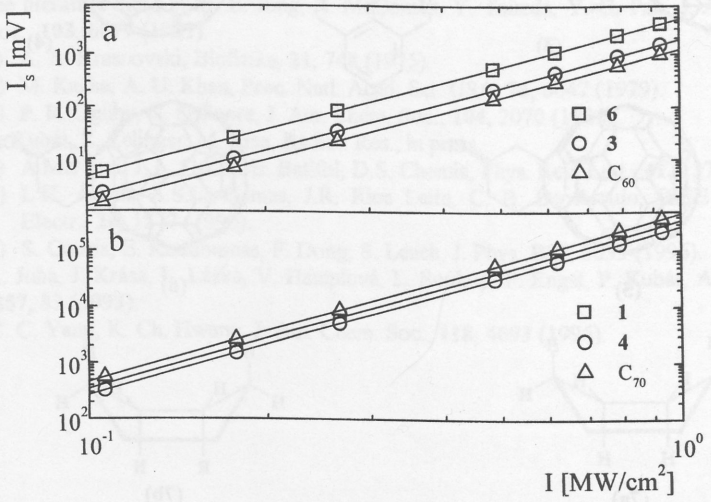

Fig. 3. Intensity dependence of the degenerate four wave mixing signal $\mathbf{k_3=2k_1-k_2}$ for a) C_{60}, **3** and **6**; b) for C_{70}, **1** and **4**

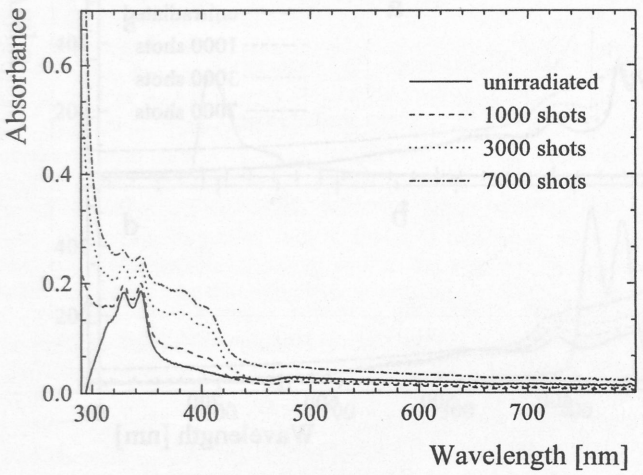

Fig. 4. UV/Vis absorption spectra of **3** in aerated toluene irradiated at 308 nm (laser pulse energy 90 mJ, intensity 3 MW cm^{-2})

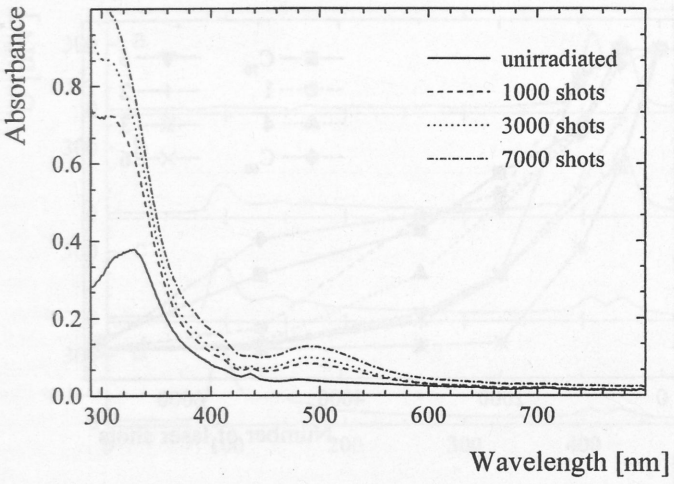

Fig. 5. UV/Vis absorption spectra of **5** in aerated toluene and irradiated at 308 nm (laser pulse energy 90 mJ, intensity 3 MW cm^{-2})

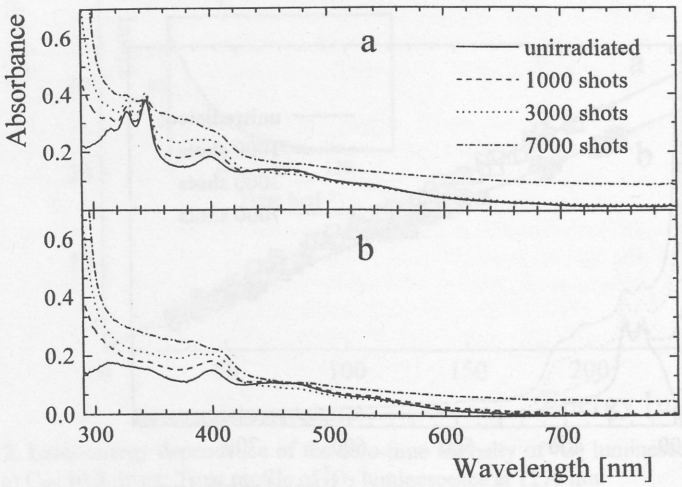

Fig. 6. UV/Vis absorption spectra of **1** (a) and **4** (b) in aerated toluene and irradiated at 308 nm (laser pulse energy 90 mJ, intensity 3 MW cm^{-2})

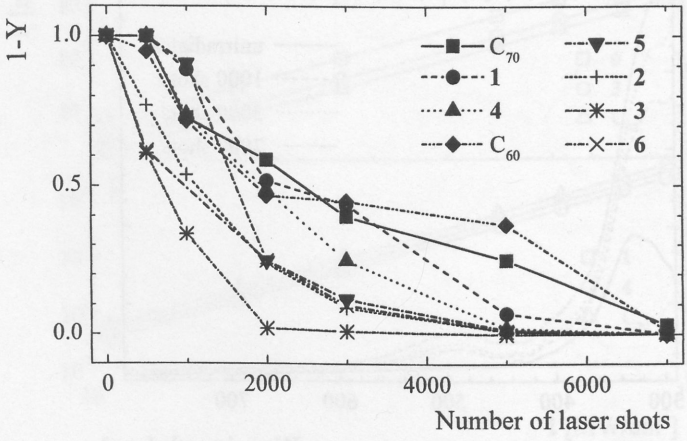

Fig. 7. Decomposition yields Y of C_{60}, C_{70}, and **1 - 6** during photolysis by XeCl laser in aerated toluene (308 nm, laser pulse energy 90 mJ, intensity 3 MW cm^{-2})

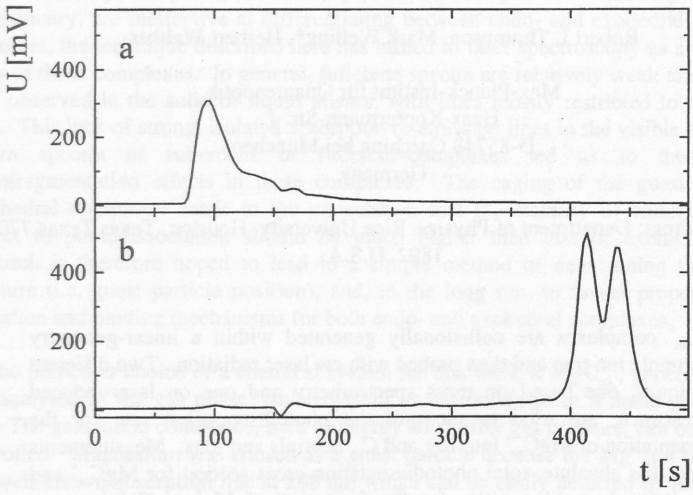

Fig. 8. Chromatograms of toluene solutions of **5** exposed to daylight for three weeks (a) and kept in the dark (b)

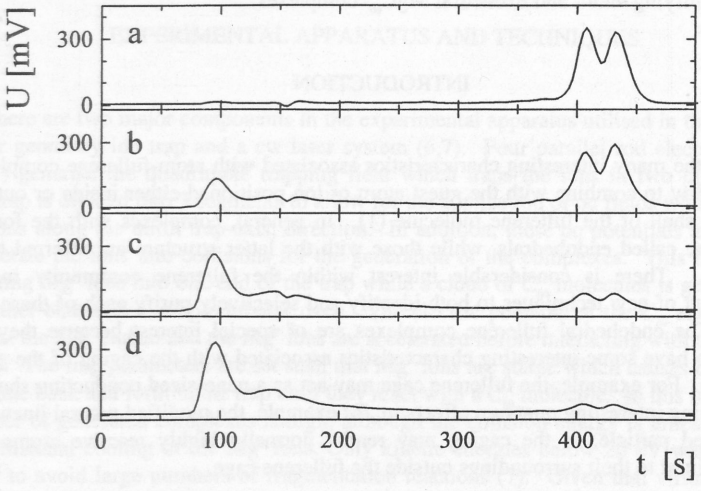

Fig. 9. Chromatograms of **5** dissolved in toluene and irradiated by 0 (a), 1000 (b), 2000 (c) and 3000 (d) laser shots (308 nm, laser pulse energy 90 mJ, intensity 3 MW cm^{-2})

STUDIES OF PHOTODISSOCIATION OF MgC_{60}^+ IN A LINEAR ION TRAP

Robert I. Thompson, Mark Welling*, Herbert Walther

Max-Planck-Institut für Quantenoptik
Hans-Kopfermann-Str. 1
D-85748 Garching bei München
Germany

*present address: Department of Physics, Rice University, Houston, Texas Texas 77005-1892, U.S.A.

MgC_{60}^+ complexes are collisionally generated within a linear-geometry quadrupole ion trap and then probed with cw laser radiation. Two different techniques, one based on mass spectrometry and one on laser-induced fluorescence, are used to measure the photodissociation rate for the fragmentation of MgC_{60}^+ into Mg and C_{60} neutrals and ions. Measurements of both the absolute, total photodissociation cross-section for MgC_{60}^+ and the relative branching ratios for the formation of Mg^+ or C_{60}^+ ions are presented. The dependence of the cross-section on wavelength in the visible and ultra-violet wavelength regions are discussed with respect to the possibilities for using photodissociation measurements as a tool for identifying endo- and exohedral MgC_{60}^+ complexes

INTRODUCTION

One of the many interesting characteristics associated with atom-fullerene complexes is their ability to combine with the guest atom or ion positioned either inside or outside the carbon shell of the fullerene molecule (1). In general, complexes with the former structure are called endohedrals, while those with the latter structure are referred to as exohedrals. There is considerable interest within the fullerene community in the development of new techniques to both identify and selectively purify each of these two species. The endohedral fullerene complexes are of special interest because they are expected to have some interesting characteristics associated with the caging of the guest particle (2). For example, the fullerene cage may act as a nano-sized conducting shell or cavity causing interesting quantum effects in, for example, the modified natural linewidth of a trapped particle, or the caging may render normally highly reactive atoms and molecules inert to their surroundings outside the fullerene cage.

Unfortunately, many common techniques for the study of fullerenes, especially mass spectrometry, are ineffective at differentiating between endo- and exohedral complexes. Therefore, the technique described here has turned to laser spectroscopy as a tool for the study of these complexes. In general, fullerene spectra are relatively weak and have only been observed in the solid or liquid phases, with lines mostly restricted to the infrared (3,4). This lack of strong, isolated absorption or emission lines in the visible range in the known spectra of fullerenes or fullerene-complexes led us to the study of photofragmentation effects in these complexes. The caging of the guest particle in endohedral complexes leads to the expectation that the stability of endohedrals with respect to photodissociation should be much higher than that of exohedrals. This approach is therefore hoped to lead to a simple method of determining the complex structure (i.e. guest particle position), and, in the long run, to reveal properties of the formation and binding mechanisms for both endo- and exohedral complexes.

The particular choice of a chemical system for this work is MgC_{60}^{+}, generated, stored, and analysed in the gas phase, isolated from its surroundings in a linear-geometry ion trap. The generation conditions, such as energy and buffer gas pressure, can be accurately controlled. Magnesium was chosen as a guest particle because the Mg^{+} ion has a strong and well-known absorption line at 280 nm which can be easily detected by laser-induced fluorescence (LIF) (5). This is useful for optical alignment of the system, and it is also required for one of the techniques which will be demonstrated for the determination of the absolute, total, photodissociation cross-section of the complex (6).

EXPERIMENTAL APPARATUS AND TECHNIQUES

There are two major components in the experimental apparatus utilised in this work: a linear geometry ion trap and a cw laser system (6,7). Four parallel rod electrodes (see Fig.1) generate the quadrupole trapping field which traps the ions in two dimensions. The trap is divided into 3 segments to allow for the application of dc fields which contain the ions along the third, trap-axis, direction. In addition, these dc potentials are used to accelerate the ions into collisions for the generation of the complexes. This is done by injecting Mg^{+} ions into one end of the trap while a cloud of C_{60} molecules is generated at the other end with a simple tubular oven. The electric potential at the C_{60} end is lower than at the Mg^{+} end so that the Mg^{+} ions are accelerated before interacting with the neutral cloud. The trap parameters are set such that Mg^{+} ions are stable which causes the ions to oscillate back and forth in the trap until they react with a C_{60} molecule. In this manner the number of generated complexes is high, although the collision energy is unresolved due to collisional cooling of the Mg^{+} ions. Only kinetic energies below 20 eV were used in order to avoid large numbers of fragmentation reactions (7). Given that virtually all of the trapping parameters are mass dependent (8), the ion trap itself acts as a mass spectrometer. Specifically, a second quadrupole field resonantly excites the mass

dependent secular motion of the ions in the trapping field. This causes the amplitude of the ion motion to increase until it can be pulled out of the trap and detected with a biased electron multiplier tube. With this technique, we have observed mass resolutions as high as $m/\Delta m=800$. The ion trap and fullerene-complex generation procedure are described in more detail in another paper in this volume (7).

The probe laser beams are generated via a series of different but related laser sources. An argon ion laser was used to pump an actively stabilised cw ring dye laser. The dye laser provided wavelengths between 536 and 594 nm while the argon ion laser itself has several useful lines between 458 and 514 nm. The dye-laser output was doubled with a KDP crystal in an external intensity enhancement cavity to provide coherent radiation near 280 nm. Finally HeNe and diode lasers were used to provide radiation at 633 and 1300 nm. The employed laser powers were in general always at or below 10 mW.

The first approach to the measurement of laser-induced photodissociation rates was to use mass spectrometry to monitor the populations of the trapped ion species (MgC_{60}^+ and C_{60}^+) as a function of laser exposure time. The laser beams passed through the interaction region at the centre of the trap at an angle of 15° to the trap axis (Fig. 1). Computer control was used to repeatable load similar samples of MgC_{60}^+ into the trap. After each loading the sample was exposed to laser radiation with well defined intensity for a certain period of time and then a mass spectrum was taken, before the trap was reloaded. By taking these spectra at several different exposure times the exponential decay of the MgC_{60}^+ complexes was observed (Fig.2a). The second and complementary technique observed the generation of Mg^+ product ions rather than the destruction of the reactants. In addition to the usual dissociating laser, a second, low intensity (Power < 1 mW), co-linear, chopped laser beam at 280 nm was used to probe the sample. After initially removing all Mg^+ ions from the trap, the fluorescence from the liberated Mg^+ ions was monitored as a function of time and the photodissociation rate was determined from the $(1-e^{-Rt})$ curve (Fig. 2b). The probe laser was attenuated and chopped to minimise any photodissociation due to the 280 nm radiation.

RESULTS AND DISCUSSION

Measurements of the dissociation rate R by either technique described above can be made at different values of laser power and wavelength. Measurements of the rate as a function of laser power revealed a linear dependence up to our maximum power of 50 mW (Intensity = 320 W/cm^2), indicating that at these low power levels only single photon processes are observed. Therefore, the linear photodissociation cross-section σ, which is a characteristic of the molecule, can be calculated from the rate by application of

$$R = \frac{I_L}{h\nu}\sigma, \qquad [1]$$

where I_L is the average light intensity incident on a trapped molecular complex, and $h\nu$ is the energy of a photon. In order to obtain the absolute cross-section special care must be taken to account for the fractional overlap of the laser beam with the trapping volume. The long exposure times (a second and longer) mean that at room temperature each complex passes through the exposed volume multiple times thus one need only calculate the fraction of the volume which is exposed to the laser radiation and scale the incident intensity by this factor to determine the average intensity I_L. A simple model assuming that the trapping region and laser beams are cylinders of radii ρ and w_o respectively, which overlap at an angle of 15° yields

$$\sigma = Rh\nu\frac{1}{I_L} = \frac{\pi hc\rho L}{8.0}\frac{R}{\lambda P_o} = \gamma(\rho, L)\frac{R}{\lambda P_o}, \qquad [2]$$

where L is the trap length and P_o is the incident laser power. Note that under these conditions the rate R is dependent on the laser power P_o, not the intensity. This results from the fact that, when the intensity is increased by tightening the focusing, the fraction of time that a molecule is exposed to the radiation decreases with exactly the same dependence that the intensity increases. Thus as long as the process is first order, it is power dependent and not intensity dependent. More exact calculations based on calculated ion distributions and a gaussian intensity distribution of the laser beam reveal a similar result, and for our experimental conditions γ=1.2 x 10^{-17} $cm^2 \cdot s \cdot mW \cdot \mu m$. In addition, these calculations were used to determine an error budget of ±18% on the absolute cross-section values, mainly resulting from the uncertainty in the ion cloud temperature. The absolute, total, photodissociation cross-sections for MgC_{60}^+ were determined at selected wavelengths between 280 and 633 nm, with incident laser powers of 3 to 11 mW and are shown in Fig. 3. An attempt was made to measure the cross-section at 1.3 μm, but no measurable dissociation was observed and only an upper bound of ~8 x 10^{-21} cm^2 could be determined.

Given the low collision energies (~10 eV) at which the complexes were generated, it is expected that most of these complexes are exohedral in nature (1,9), and this data provides two clear indications that this is indeed the case. First, the observation of reasonably rapid, single-photon fragmentation at the employed wavelengths (photon energy < 4.5 eV) suggests exohedral complexes because the energy required to pass a large atom through the cage to form an endohedral is over 20 eV (1,10), and positively charged guest ions make the complex even more stable (11). Therefore, one would not

expect to observe this much fragmentation of endohedrals at these low photon energies. Second, and more concrete, the very slow increase of the cross-section with photon energy may be fitted with a broad gaussian function (Fig. 3). This is similar to the energy dependence observed when a molecule dissociates by a transition from a bound lower state to the turning point of a repulsive upper state in which the Franck-Condon factor in the reaction rate is simply a mapping of the ground state wavefunction onto photon-energy space (Fig.4a). This is a reasonable explanation of what may be happening with exohedral MgC_{60}^{+}, although endohedrals would be expected to have a sharp cut-off frequency to their cross-section versus photon-energy plot (Fig.4b) which occurs when the photon energy becomes too low to excite the atom above the height of the potential barrier formed by the C_{60} cage. In the case of MgC_{60}^{+} the width of a sharp feature can be roughly estimated by a calculation of the rotational broadening of MgC_{60}^{+} near room temperature, which is 10 meV or less. Therefore, this data clearly suggests that these relatively quickly dissociating complexes are exohedral in nature. The total absorbance of the ground to excited state transition can be estimated by integrating the Gaussian fit to our data, and from this it is trivial to calculate the oscillator strength of the transition. In this case, it was slightly below 1, supporting the interpretation of the data as a unimolecular decay via a single electric dipole transition. This two state model is a necessary condition for the preceding analysis to hold. It should be noted that the good agreement of our data with a unimolecular decay model is a somewhat novel result as much of the previous work on photofragmentation of fullerenes (e.g. (12)) were successfully interpreted in terms of thermionic emission. However, this earlier work tended to study fragmentation of the cage itself rather than liberation of a guest atom. Nevertheless, with our present experimental apparatus, we cannot completely rule out the possibility of thermionic effects in the photodissociation of MgC_{60}^{+}.

A second class of experiments was carried out to examine the branching ratios of the different photon-induced unimolecular reaction pathways. When complexes are loaded into the trap, two species dominate, MgC_{60}^{+} and C_{60}^{+}. Secular excitation was employed to remove most of the C_{60}^{+} complexes from the trap before laser exposure. It was then possible to observe the rate of C_{60}^{+} generation as MgC_{60}^{+} was photofragmented by 280 nm radiation. The results indicated that 77 ± 9 % of the fragmented MgC_{60}^{+} appeared in the trap as C_{60}^{+} following the reaction:

$$MgC_{60}^{+} + h\nu \rightarrow Mg + C_{60}^{+}. \qquad [3]$$

There are three other possible reaction paths that the fragmentation could follow. First, it is possible that the complex could fragment into smaller fullerene fragments, but when the mass range from C_{50} to C_{59} was monitored, no significant population increase was observed. The other two possible reaction paths are:

$$MgC_{60}^{+} + h\nu \rightarrow Mg^{+} + C_{60} \quad [4]$$

$$MgC_{60}^{+} + h\nu \rightarrow MgC_{60}^{2+} + e^{-} \quad . \quad [5]$$

The fact that most reactions follow path 3 is not surprising given that the ionisation potential of Mg (13) is 75 meV higher than that of C_{60} (14) and thus path 3 is the energetically more favourable one. The presence of a significant branch following path 4 is confirmed by the increase in Mg^{+} fluorescence during the dissociation process. However, at present we cannot generate a absolute fraction from this fluorescence measurement. Therefore, a process of elimination of the other paths is employed. With respect to path 5, no formation of doubly charged product ions was detected with our system. This result can be explained by calculating a lower bound on the required photon energy for this process from the potential energy required to displace an electron from a doubly charged complex from 3.5 Å to ∞. This value turns out to be ≈8eV, thus a 4.5 eV photon (λ=280 nm) is too weak to initiate reaction 5. With the elimination of fullerene shell fragmentation and ionisation, the only remaining branch is path 4, which therefore has a probability of 23%.

The most recent experimental results employed longer laser exposures to further investigate the influence of the He buffer gas in the formation process. The results have shown that under some formation conditions, there appear to be two different species at the MgC_{60}^{+} mass in the trap. Under 280 nm laser exposure, the photodissociation curve contains two different exponentially decaying fractions, with the slower decaying fraction having a lifetime of a factor of at least 30 times larger than the originally observed species (Fig. 5). The original, fast decaying species is still present and forms at least 60% of the complexes generated under any collision conditions. The fraction of the samples which decays slowly is nonlinearly dependent on the collision energy and the buffer gas pressure, with the slowly-dissociating fraction dropping to zero at low values of either quantity. The former result indicates that only the higher energy ions generated by the ion source actually form these slow dissociating complexes. Most of the kinetic energy from an incident Mg^{+} ion is converted into internal energy after capture, and must be somehow removed before the complex breaks apart. This explains the fact that the size of the slow fraction is strongly dependent on the buffer gas pressure in that the He atoms are needed to carry off the excess energy. These results support the interpretation that the more slowly dissociating fraction corresponds to more stable endohedral complexes. Further experimentation is planned to confirm this. Specifically, we hope to explore the reactivity of exohedral MgC_{60}^{+} vs endohedral MgC_{60}^{+} with the expectation of finding a lower reactivity for the endohedral complexes.

One of the goals of studying these two species is that should the slow-dissociating fraction be confirmed as an endohedral complex, then photodissociation measurements

could be used a spectroscopic identification tool to differentiate endo- and exohedral complexes. Even more important, photodissociation could be used to generate pure, gaseous samples of endohedral complexes by fragmenting the exohedrals, and then using secular excitation to remove them from the trapping volume. Virtually pure, fast dissociating complexes, thought to be exohedral complexes, can be produced simply by controlling the collision parameters (low collision energy and low buffer gas pressure).

CONCLUSIONS

This work demonstrates two experimental techniques for the measurement of absolute, total, photodissociation cross-sections as a function of photon energy by application of low laser intensities to ensure the observation of only single-photon processes. In addition, a similar technique is shown to determine the branching ratio or partial cross-section for photodissociation processes which have more than one possible reaction pathway. All of these techniques were applied to MgC_{60}^{+} complexes and the results provided insight into the formation process and structure of these complexes and opened the possibilities of using photodissociation as a tool for identification or purification of endo- and exohedral complexes.

REFERENCES

1. Y. Basir, and S.L. Anderson, Chem. Phys. Lett., **243**, 45 (1995).
2. D.S. Bethune et al., Nature, **366**, 123 (1993).
3. K. Kikuchi et al., Chem. Phys. Lett., **216**, 67 (1993).
4. H. Shinohara et al., J. Phys. Chem.,**98**,8597 (1994).
5. F. Diedrich, E Peik, J.M.Chen, W.Quint, H.Walther, Phys. Rev. Lett., **59**, 2931 (1987).
6. M. Welling, R .I. Thompson, and H. Walther, Chem. Phys. Lett., **253**, 37 (1996).
7. M. Welling, H.A. Schuessler, R.I. Thompson, and H. Walther, in Recent Advances in the Chemistry and Physics of Fullerenes and Related Materials: Vol. 4, K.M.Kadish and R.S.Ruoff, Editors, **PV 97-14**, The Electrochemical Society Proceedings Series, Pennington, NJ (1997).
8. W. Paul, Angew. Chem. (Engl. Ed.), **29**, 739 (1990).
9. L.M. Roth et al., J. Am. Chem. Soc., **113**, 6298 (1990).
10. Z. Wan, J.F. Christian, and S.L. Anderson, Phys. Rev. Lett., **69**, 1352 (1992).
11. J. Cioslowski, and E. Fleischmann, J. Chem. Phys., **94**, 3730 (1991).
12. E.E.B. Campbell, G. Ulmer, and I.V. Hertel, Phys. Rev. Lett., **67**, 1986 (1991).
13. C.E. Moore, Atomic Energy Levels, Vol. 1, Circular of the National Bureau of Standards 467, p. 106, United States Department of Commerce, Washington (1949).
14. R. K. Yoo, B. Ruscic, and J. Berkowitz, J. Chem. Phys., **96**, 911 (1992).

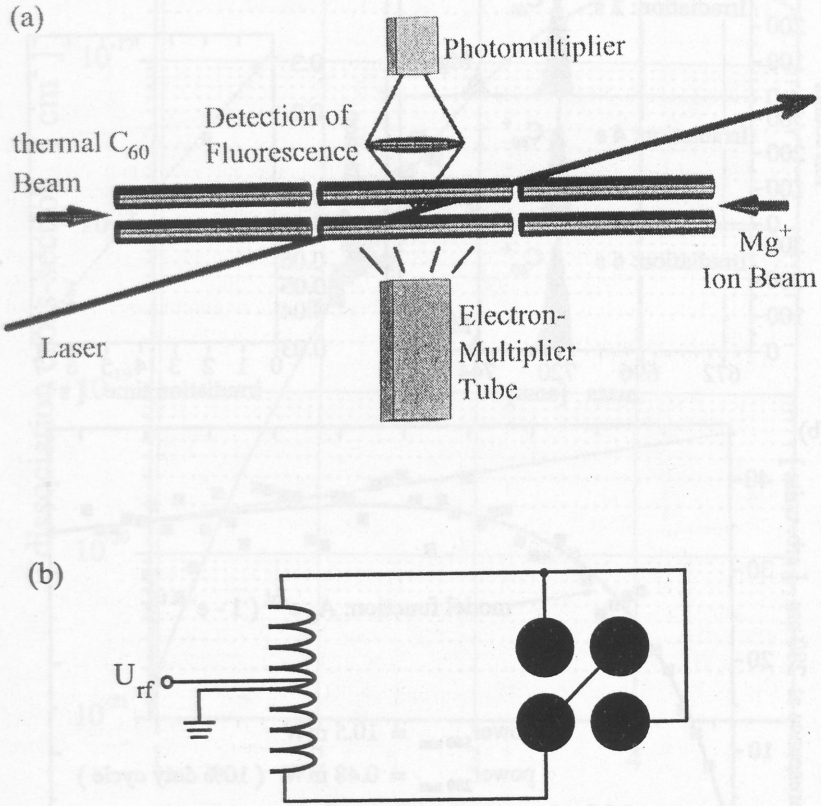

Fig. 1: Schematic diagrams of the linear-geometry ion trap including: (a) the positions of the probe laser beam, particle beams, electron multiplier tube, and photomultiplier tube and (b) the electrode arrangement used for quadrupole field generation.

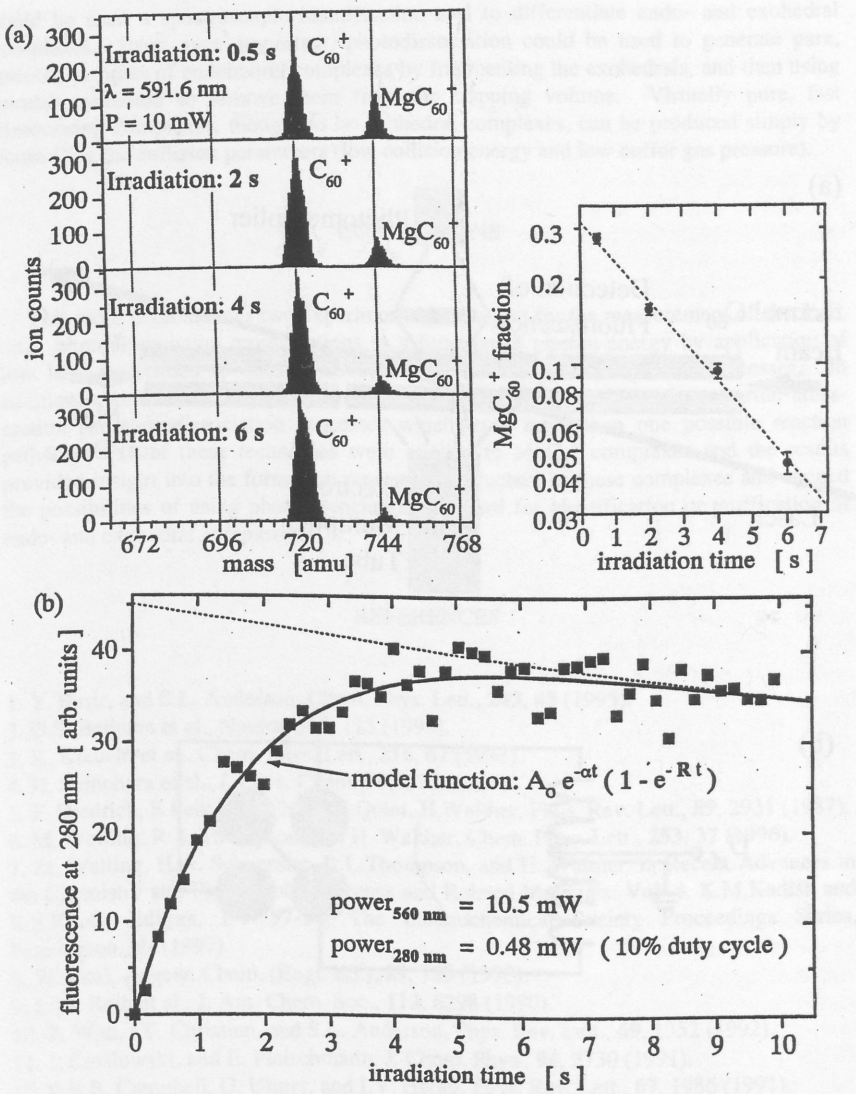

Fig. 2: Typical data curves for (a)mass spectrometric, and (b) laser-induced fluorescence techniques for the determination of photodissociation rates for MgC_{60}^{+}. The laser powers and wavelengths are shown in the Figure.

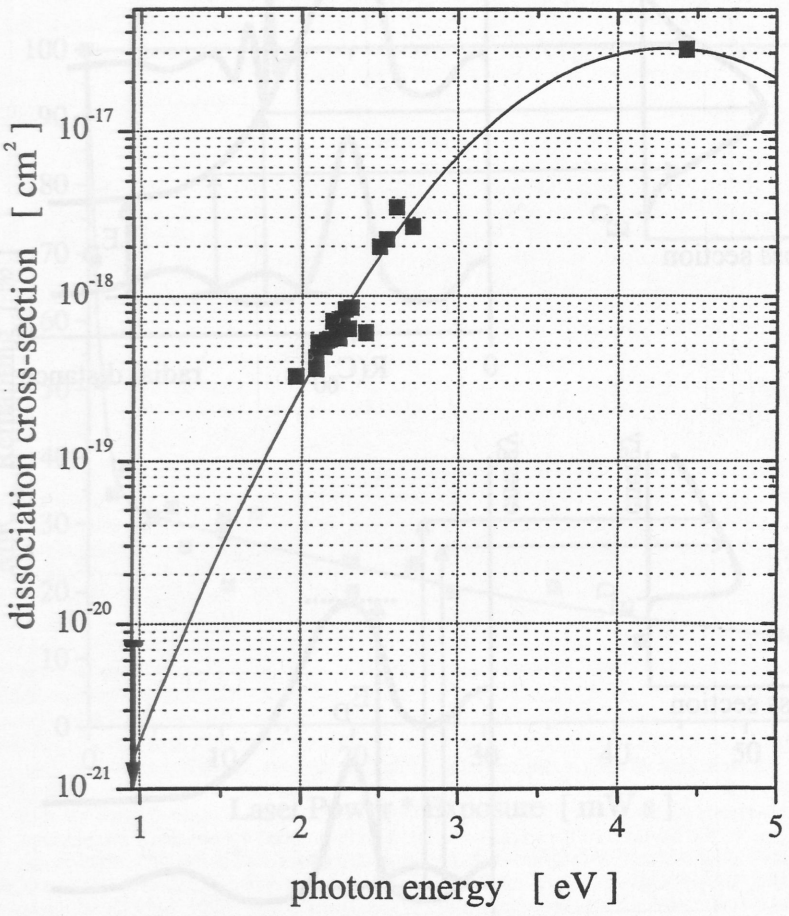

Fig. 3: Absolute, total, photodissociation cross-sections of MgC_{60}^+ as a function of photon energy, measured with incident cw-laser powers between 3 and 11 mW. The solid line is a Guassian curve fit to the data.

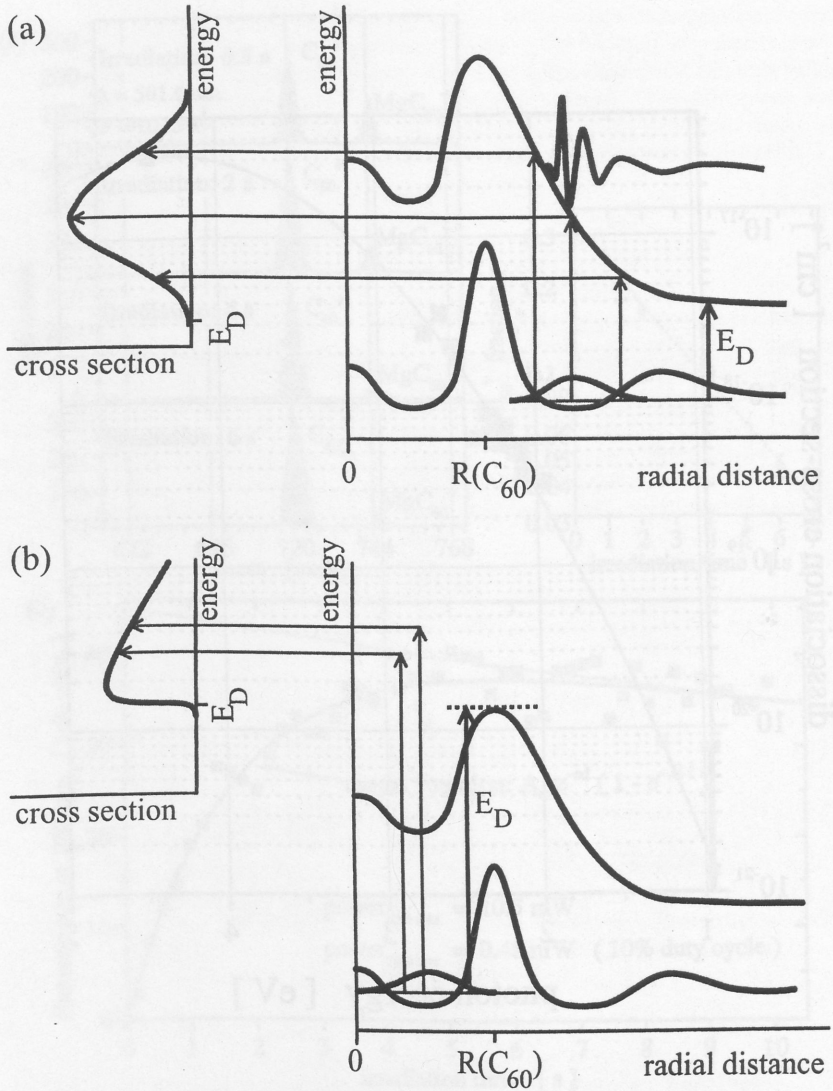

Fig. 4: Sketches of possible ground and excited state potential curves for MgC_{60}^+ and the resulting approximate dissociation cross section vs. photon energy curves for (a) endohedral and (b) exohedral complexes.

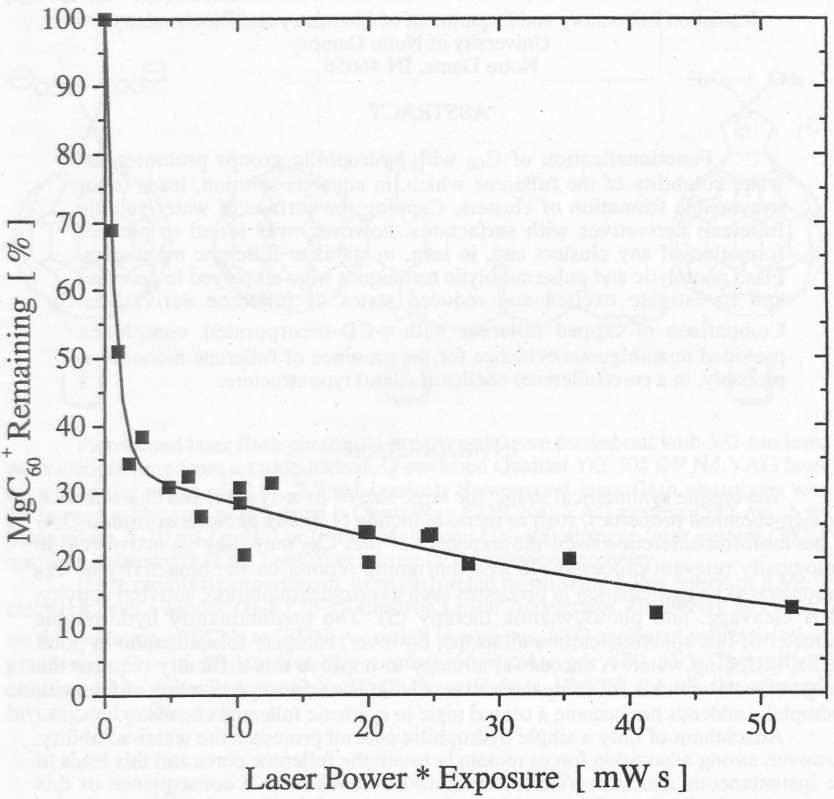

Fig. 5: Fraction of MgC_{60}^{+} complexes remaining after sample exposure to a given laser power for various times. The complexes were generated at a collision energy of 10 eV and an He buffer gas pressure of 5.5 x 10^{-6} mbar. The solid line is a two component exponential fit to the data.

FLASH PHOTOLYSIS AND PULSE RADIOLYSIS STUDIES ON WATER-SOLUBLE FULLERENE CLUSTERS AND CAPPED FULLERENES

Dirk M. Guldi* and Klaus-Dieter Asmus

Radiation Laboratory and Department of Chemistry and Biochemistry,
University of Notre Dame
Notre Dame, IN 46656

ABSTRACT

Functionalization of C_{60} with hydrophilic groups promotes the water solubility of the fullerene which, in aqueous solution, leads to an irreversible formation of clusters. Capping the surface of water-soluble fullerene derivatives with surfactants, however, was found to prevent formation of any clusters and, in turn, to stabilize fullerene monomers. Flash photolytic and pulse radiolytic techniques were employed to generate and investigate excited and reduced states of fullerene derivatives. Comparison of capped fullerene with γ-CD-incorporated complexes provided unambiguous evidence for the presence of fullerene monomers, probably, in a core(fullerene)-shell(surfactant) type structure.

INTRODUCTION

The unique symmetrical shape, the large size of its π-system, and characteristic physico-chemical properties, such as facile reduction (1,2) and photosensitization (3,4) of buckminsterfullerene raised the expectation that C_{60} may play an active role in biologically relevant processes. Indeed, intriguing reports on the bioactivity of C_{60} demonstrated its participation in processes such as enzyme inhibition, antiviral activity, DNA cleavage, and photodynamic therapy (5). The predominantly hydrophobic character of this spherical carbon allotrope, however, hampers solubilization in polar media, including water. A successful strategy to improve this difficulty requires the design of water-soluble fullerene derivatives (5-7). Thus, functionalization of C_{60} with hydrophilic addends has become a central topic in synthetic fullerene chemistry.

Attachment of only a single hydrophilic addend promotes the water-solubility. However, strong adsorption forces remain between the fullerene cores and this leads to the instantaneous and irreversible formation of clusters. As a consequence of this aggregation, the lifetime of the excited triplet state is reduced by orders of magnitudes and detectable reduction is limited to fullerene monomers (8). On the other hand, increasing the number of addends at the fullerene core, e.g. via controlled bis-, tris-, or even polyfunctionalization, and thereby lowering the fullerene's hydrophobic surface, prevents formation of colloidal fullerene clusters (9).

Surfactants have been successfully employed to solubilize pristine fullerenes in aqueous media in reasonable yields (9-11). Although the investigated derivatives are sufficiently water-soluble, it will be shown in the present investigation that utilization of cationic (cetyltrimethylammonium chloride) and nonionic (Triton X-100) detergents is crucial to cap the fullerene core and, thus, obstruct formation of colloidal fullerene clusters.

EXPERIMENTAL

Details of the synthesis of $C_{60}C(COO^-)_2$ (**1**), $C_{60}(C_9H_{11}O_2)(COO^-)$ (**2**), and $C_{60}(C_4H_{10}N^+)$ (**3**) fullerenes have been described in earlier contributions (12,13).

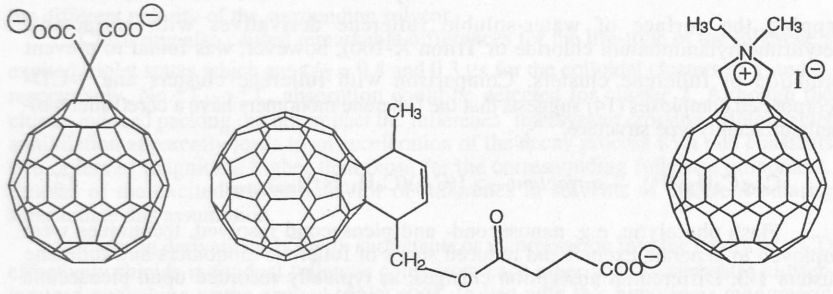

1 **2** **3**

Picosecond laser flash photolysis experiments were carried out with 532-nm laser pulses originating from a mode-locked, Q-switched Quantel YG-501 DP Nd:YAG laser system (pulse width ≈ 18 ps, 2-3 mJ / pulse). Nanosecond laser flash photolysis was performed with laser pulses from a Qunta-Ray CDR Nd: YAG system (532 nm, 6 ns pulse width, 5-10 mJ / pulse) or from a Molectron UV-400 nitrogen laser system (337.1 nm, 8 ns pulse width, 1 mJ / pulse) in a front face excitation geometry.

Pulse radiolysis experiments were performed by utilizing 50-ns pulses of 8 MeV electrons from a Model TB-8 / 16-1S Electron Linear Accelerator. Dosimetry was based on the oxidation of SCN^- to $(SCN)_2^{\bullet -}$, which in aqueous, N_2O-saturated solutions takes place with G ≈ 6 (G denotes the number of species per 100 eV). The radical concentration generated per pulse amounts to (1-3) x 10^{-6} M for all the systems investigated in this study.

RESULTS AND DISCUSSION

A promising approach to overcome the water insolubility of pristine fullerenes encompasses amphiphilic functionalization of pristine C_{60} via covalent attachment of hydrophilic addends (5-7). Functionalization of C_{60} with hydrophilic addends, such as carboxyl groups or quartery ammonium cations successfully promotes the water solubility of the fullerene core.

Dissolving fullerene derivatives **1-3** in aqueous solution, via suspension in tetrahydrofuran (THF) and subsequent addition of water, leads in general to the irreversible formation of fullerene clusters. This was followed spectroscopically, e.g. the sharp absorption bands of monomeric fullerenes (for example $C_{60}(C_4H_{10}N^+)$ **3**: 215, 258, 310, 416, 524, and 699 nm) transform into broadly absorbing features (around 263, 332, and 435 nm). These spectral differences serve as a sensitive marker for colloidal C_{60} clusters and resemble those of pristine C_{60} in polar or vesicular media.

The data presented here on the functionalization of C_{60} show that a single hydrophilic addend is not sufficient to prevent the strong hydrophobic 3-dimensional interactions among the fullerene moieties and the resulting tendency to form aggregates. This precludes, formation of stable monomers of monofunctionalized fullerene derivatives in aqueous solution and leads to the irreversible formation of clusters.

$$C_{60}(C_4H_{10}N^+) \quad \text{—}aqueous\ solution\text{—>} \quad \{C_{60}(C_4H_{10}N^+)\}_n \qquad (1)$$

Capping the surface of water-soluble fullerene derivatives with surfactants (cetyltrimethylammonium chloride or Triton X-100), however, was found to prevent formation of fullerene clusters. Comparison with fullerene clusters and γ-CD-incorporated complexes (14) suggests that the fullerene monomers have a core(fullerene)-shell(surfactant) type structure.

$$C_{60}(C_4H_{10}N^+) \quad \text{—}surfactant\text{—>} \quad [(C_{60})(C_4H_{10}N^+)]_{surfactant} \qquad (2)$$

Flash photolytic, e.g. nanosecond- and picosecond resolved, techniques were employed to generate excited and reduced states of fullerene monomers and fullerene clusters **1-3**. Differential absorption changes, as typically recorded upon picosecond excitation, revealed spectral characteristics of the respective $^*S_1 \text{->} ^*S_n$ absorptions which were found to be independent on the aggregation state, e.g. monomer versus cluster.

$$\{C_{60}(C_4H_{10}N^+)\}_n \text{—}h\nu\text{—>} \{^1C_{60}(C_4H_{10}N^+)\}_n$$
$$\text{—}ISC\text{—>} \{^3C_{60}(C_4H_{10}N^+)\}_n \qquad (3)$$

Table 1: Photophysical data of fullerene clusters 1-3 in aqueous media as derived from picosecond measurements.

Compound	λ_{max} ($^1C_{60}$)R [nm]	λ_{max} ($^3C_{60}$)R [nm]	Inter System Crossing (ISC)	$\tau_{1/2}$ ($^3C_{60}$)R
$\{C_{60}C(COO^-)_2\}_n$ **(1)**	888	706	1.2 ns	0.4 μs
$\{C_{60}(C_9H_{11}O_2)(COO^-)\}_n$ **(2)**	910	690	1.4 ns	[a]
$\{C_{60}(C_4H_{10}N^+))\}_n$ **(3)**	920	680	1.3 ns	0.3 μs

[a] no observable absorption changes upon nanosecond pulse

The intersystem crossing rates to the excited triplet state for fullerene clusters **1-3** closely resemble those of various monofunctionalized fullerene derivatives in non-polar solutions. This is remarkable, since closely packed thin films of C_{60}, as formed upon sublimation, display a much faster decay on the order of 2 ps for the fullerenes excited singlet state. This density dependence of the relaxation process has been interpreted in terms of a fast depopulation of the excited singlet state via singlet-singlet annihilation. Since unambiguous evidence substantiates the cluster concept of compounds **1-3**, the present data suggest relatively weaker cohesive interaction between the fullerene moieties in aqueous solutions than in thin films. This is interesting in the sense that, on an absolute scale, the cohesive forces in the cluster are, nevertheless, strong enough to prevent easy redissolution. In conclusion, fullerene aggregation was found to have insignificant impact on those physico chemical properties which are related to the

generation and fate of the fullerene's excited singlet state.

Noticeable differences were observed with respect to the absorption maxima of the corresponding $^*T_1 \rightarrow ^*T_n$ absorptions for monomeric and colloidal derivatives **1-3** in nanosecond studies (15,16). In surfactant media, the maxima were generally blue-shifted relative to the analogous γ-CD complexes, e.g., $[(^3C_{60})(C_4H_{10}N^+)]_{surfactant}$: 690 nm *vs* $[(^3C_{60})(C_4H_{10}N^+)]$/γ-CD: 700 nm. These shifts parallel the blue-shifts of the fullerene clusters ($\{C_{60}(C_4H_{10}N^+)\}_n$: 680 nm). A possible rationale for this observation may be the different polarity of the surrounding solvent.

Clustering also caused remarkable differences for the life-time of the fullerene's excited triplet states which are $\tau_{1/2}$ = 0.4 and 0.3 μs for the colloidal clusters of **1** and **3**, respectively. No $^*T_1 \rightarrow ^*T_n$ absorption could be detected for cluster **2**. Although the cluster-induced packing did not impact the fullerenes' intersystem crossing, triplet-triplet annihilation apparently leads to an acceleration of the decay process with rate constants two orders of magnitude higher than those for the corresponding fullerene monomers. Studies of the excited triplet behavior of fullerenes in solvents of different polarity substantiate this assumption.

Capping derivatives **1-3** with surfactants or incorporation into the cavity of γ-CD effectively shields individual fullerene cores from each other and discriminates cluster-induced quenching of the excited triplet state. In line with this hypothesis monomeric derivatives **1-3** revealed the instantaneous formation of long lived $^*T_1 \rightarrow ^*T_n$ absorptions with life-times exceeding those observed in homogeneous solutions. Exponential decay to the original base line, as observed in the time-absorption profiles throughout the UV-vis-NIR range indicates no noticeable chemical reaction of the photoexcited fullerenes with the surfactant or γ-CD host.

Table 2: Photophysical data of monomeric fullerene / surfactant complexes 1-3 in aqueous media.

Compound	λ_{max} $(^3C_{60})$R [nm]	$\tau_{1/2}$ $(^3C_{60})$R	$k_{quenching}$ (DABCO) $[M^{-1}s^{-1}]$	$\tau_{1/2}$ $(C_{60}^{\bullet-})$R
$[C_{60}]_{surfactant}$ [a]	750		7.4×10^7 [a]	0.44 ms
$[C_{60}C(COO^-)_2]_{surfactant}$ **(1)**	700	69 μs	4.8×10^6	1.1 ms
$[C_{60}(C_9H_{11}O_2)(COO^-)]_{surfactant}$ **(2)**	690	63 μs	4.9×10^6	2.4 ms
$[C_{60}(C_4H_{10}N^+)]_{surfactant}$ **(3)**[a]	690	56 μs	7.8×10^6	1.9 ms

[a] counter anion is chloride

Reductive quenching of the fullerenes' excited triplet state with sacrificial electron donors, such as DABCO, was achieved by photoexcitation of solutions of monomeric derivatives **1-3**.

$$[(^3C_{60})(C_4H_{10}N^+)]_{surfactant} + \text{DABCO} \longrightarrow [(C_{60}^{\bullet-})(C_4H_{10}N^+)]_{surfactant} + (\text{DABCO})^{\bullet+} \quad (4)$$

The higher electron withdrawing effects induced by the functional groups in derivatives **1** and **2**, as compared to the quartery ammonium cation in $C_{60}(C_4H_{10}N^+)$ **3**, lead to a two-fold decrease of the underlying quenching rate constant. In γ-CD complexes, the rates for

charge-recombination were found to be on the order of 2 x 10^4 s^{-1} (not listed), indicating a destabilization of the charge separated radical pair by nearly two-orders of magnitude relative to the analogous capped derivatives (~ 3 x 10^2 s^{-1}). These trends are well in line with pristine C_{60} and can be considered to reflect a more proficient penetration of DABCO molecules towards the photoexcited fullerene, namely ($^3C_{60}$)R, in the cavity of the γ-CD host than through the surfactant shell. In turn, charge recombination, by means of a reaction between $(DABCO)^{\bullet+}$ and ($C_{60}^{\bullet-}$)R, should be similarly affected.

Pulse radiolysis is another important source for fast kinetic spectroscopic studies and for the generation of π-radical anions of pristine fullerenes and functionalized fullerene derivatives. As a consequence of the moderate redox potential of pristine C_{60} radical-induced reduction by hydrated electrons or $(CH_3)_2{}^{\bullet}C(OH)$ radicals take place rapidly (17). Surprisingly, pulse radiolysis experiments failed to substantiate any reduction of compounds **1** and **2** in aqueous solution. The decay of the hydrated electron at 720 nm was virtually unaffected regardless of the applied fullerene concentration. The lack of any detectable absorption changes in the NIR, which are attributable to the fullerene π-radical anion ($C_{60}^{\bullet-}$), further corroborates this observation, and was rationalized in terms of clustering (13).

Differential absorption changes at 720 nm (absorption maximum of the hydrated electron) and throughout the NIR, recorded upon pulse radiolysis of surfactant capped **2** in deoxygenated aqueous/2-propanol solution (9:1 v/v) confirm that this fullerene monomer is susceptible for reduction. Variation of the concentration (0.2 - 4.0 x 10^{-5} M) impacted the decay of the hydrated electron absorption at 720 nm in a linear manner. The underlying rate was found to be dependent on the fullerene concentration and, furthermore, in excellent agreement with the rate of formation of the fullerene π-radical anion (1015 nm). This suggests that the observed reaction can be unambiguously ascribed to reduction of the fullerene complex by hydrated electrons.

$$[C_{60}(C_4H_{10}N^+)]_{surfactant} + e_{aq}^- \longrightarrow [(C_{60}^{\bullet-})(C_4H_{10}N^+)]_{surfactant} \quad (5)$$

$$[C_{60}(C_4H_{10}N^+)]_{surfactant} + (CH_3)_2{}^{\bullet}C(OH) \longrightarrow [(C_{60}^{\bullet-})(C_4H_{10}N^+)]_{surfactant} + (CH_3)_2CO + H^+ \quad (6)$$

Table 3: Rate constant ($k_{reduction}$) and absorption maxima (λ_{max}) for the radiolytic reduction of monomeric fullerene / surfactant complexes 1-3 in aqueous media.

Compound	$k_{reduction}$ (e_{aq}^-) [$M^{-1}s^{-1}$]	$k_{reduction}$ ($(CH_3)_2{}^{\bullet}C(OH)$) [$M^{-1}s^{-1}$]	λ_{max} ($C_{60}^{\bullet-}$)R [nm]
$[C_{60}C(COO^-)_2]_{surfactant}$ **(1)**	1.7 x 10^{10}	5.4 x 10^8	1015
$[C_{60}(C_9H_{11}O_2)(COO^-)]_{surfactant}$ **(2)**	2.3 x 10^{10}	6.1 x 10^8	1010
$[C_{60}(C_4H_{10}N^+))]_{surfactant}$ **(3)**	3.5 x 10^{10}	7.7 x 10^8	1010

The corresponding rate constants for the reduction of $[C_{60}(C_4H_{10}N^+)]_{surfactant}$ and, as earlier reported, for $C_{60}(C_4H_{10}N^+)]$/γ-CD by hydrated electrons show a significant rate enhancement over pristine C_{60} and negatively charged analogues of **1** and

2, which were surface capped or γ-CD-incorporated. This can plausibly be rationalized in terms of the Columbic forces which decelerate a reaction between hydrated electrons and the negatively charged fullerenes while they facilitate reduction of the positively charged fullerene. On the other hand, electron transfer rates from uncharged $(CH_3)_2{}^{\bullet}C(OH)$ radicals, which should be less affected by the surface charge of the respective functionalized fullerene derivative, substantiates the trend observed for reactions of the hydrated electron. This suggests, in line with the quenching rates, an anodic shift of the reduction potential of **3** relative to **1** and **2**.

Similar to the $*T_1 \rightarrow *T_n$ absorption, NIR bands of pulse radiolytically generated π-radical anions **1-3** are very sensitive to the surrounding environment. The overall trend (see Table 3), e.g. $[(C_{60}{}^{\bullet-})(C_4H_{10}N^+)]/\gamma\text{-CD} > [(C_{60}{}^{\bullet-})(C_3H_7N)] > [(C_{60}{}^{\bullet-})(C_4H_{10}N^+)]_{surfactant} > ([(C_{60}{}^{\bullet-})(C_4H_{10}N^+)]_n$, substantiates the above observation on the maxima of the corresponding $*T_1 \rightarrow *T_n$ absorption. This leads to the hypothesis that inside of the γ-CD cavity the fullerene moiety is efficiently shielded from the aqueous phase, comparable to the environmental parameters of N-methylfulleropyrrolidine in toluene. In surfactant based core(fullerene)-shell(surfactant) structures the dynamic exchange of surfactant molecules allows contact with the surrounding aqueous phase and, thus, alters the environment of the fullerene core. Further support for this assumption emerges from studies on the radiolytic formation of equatorial-$(C_{60}{}^{\bullet-})[C(COOEt)_2]_2$ in non-polar toluene and its hydrolyzed analogue, i.e. equatorial-$(C_{60}{}^{\bullet-})[C(COO^-)_2]_2$, in aqueous media (9). The latter exhibits a bathochromic shift from 1065 nm to 1050 nm, respectively.

ACKNOWLEDGMENT

This work was supported by the Office of Basic Energy Sciences of the Department of Energy (this is contribution No. NDRL-3996 from the Notre Dame Radiation Laboratory).

REFERENCES

1. C. Jehoulet, A.J. Bard and F. Wudl, J. Am. Chem. Soc. **113**, 5456 (1991).
2. F. Zhou, C. Jehoulet and A.J. Bard, J. Am. Chem. Soc. **114**, 11004 (1992).
3. C.S. Foote, Top. in Curr. Chem. **169**, 348 (1994).
4. J.W. Arbogast and C.S. Foote, J. Am. Chem. Soc. **113**, 8886 (1991).
5. F. Diederich and C. Thilgen, Science **271**, 317 (1996).
6. A.W. Jensen, S.R. Wilson and D.I. Schuster, Bioorg. Med. Chem. **4**, 767 (1996).
7. A. Hirsch, Synthesis 895 (1996).
8. D.M. Guldi, H. Hungerbühler and K.-D. Asmus, J. Phys. Chem. **99**, 13487 (1995).
9. D.M. Guldi, Res. Chem. Inter. 1997, in press.
10. Y.N. Yamakoshi, T. Yagami, K. Fukuhara, S. Sueyoshi and N. Miyata, J. Chem. Soc., Chem. Commun. 517 (1994).
11. A. Beeby, J. Eastoe and R.K. Heenan, J. Chem. Soc., Chem. Commun. 173 (1994).
12. I. Lamparth and A. Hirsch, J. Chem. Soc., Chem. Commun. 1727 (1994).
13. D.M. Guldi, H. Hungerbühler and K.D. Asmus, J. Phys. Chem. A **101**, 1783 (1997).
14. T. Andersson, K. Nilsson, M. Sundahl, G. Westman and O.J. Wennerström, Chem. Soc., Chem. Commun. 604 (1992).

15. J.L. Anderson, Y.Z. An, Y. Rubin and C.S. Foote, J. Am. Chem. Soc. **116**, 9763 (1994).
16. R.M. Williams, J.M. Zwier and J.W. Verhoeven, J. Am. Chem. Soc. **117**, 4093 (1995).
17. D.M.Guldi, H. Hungerbühler, E. Janata and K.-D. Asmus, J. Chem. Soc., Chem. Commun. 84 (1993).

PHOTOINDUCED ELECTRON TRANSFER IN SUPRAMOLECULAR RUTHENIUM (II) / C_{60} DYADS

Dirk M. Guldi*,
Radiation Laboratory, University of Notre Dame, Notre Dame, IN 46656
U.S.A.
Michele Maggini, Simonetta Mondini, Gianfranco Scorrano
Centro Meccanismi CNR, Dipartimento di Chimica Organica,
Via Marzolo 1, 35131 Padova, Italy
Maurizio Prato
Dipartimento di Scienze Farmaceutiche, Università di Trieste, Piazzale
Europa 1, 34127 Trieste, Italy

ABSTRACT

Excited states properties of two supramolecular Ru(II)-C_{60} donor-bridge-acceptor dyads were studied under various conditions and compared to those of a model complex Ru(II)$(bpy)_2$(bpy-R). The steady-state luminescence yield of Ru(II)-C_{60} dyads is noticeably quenched relative to the ruthenium model complex indicating intramolecular electron/energy transfer from the ruthenium excited MLCT state to the fullerene's ground state. Picosecond resolved photolysis shows that the photoexcited MLCT state in the Ru(II)-C_{60} dyad transforms rapidly into the charge separated state (Ru(III)-$C_{60}^{\bullet-}$) which was confirmed by monitoring the characteristic NIR absorption of the fullerene π-radical anion.

INTRODUCTION

Photoexcited states of ruthenium polypyridyl complexes and its derivatives have evoked interdisciplinary interest to employ them as building blocks in devices that perform light- and/or redox-induced functions (1). The strong emission of the ruthenium's metal-to-ligand charge transfer states, generated with high quantum yields, make these long-lived states attractive and convenient probes for monitoring energy and electron transfer processes. The remarkable redox features of pristine fullerenes and monofunctionalized fullerene derivatives, in their ground ($E_{1/2}$ (= –0.44 V vs SCE) and also photoexcited states ($E_{1/2}$ ($^1C_{60}$) = + 1.44 V vs SCE; $E_{1/2}$ ($^3C_{60}$) = + 1.01 V vs SCE) (2), suggests that they are potentially useful as electron acceptor moieties in supramolecular electron relay systems. Accordingly the unique combination of photosensitive ruthenium-(II) complexes with electron-deficient fullerenes is a promising approach for photosensitive assemblies (3). This inspired us to extend our concept of donor-bridge-acceptor dyads for the design of light-harvesting devices and to investigate them in electron transfer reactions.

The energetically high-lying ruthenium excited MLCT state ($E_{0-->0}$ = 1.96 eV) (1) should facilitate photoinduced intramolecular electron transfer to the fullerene's ground state.